FOREX Publication
Open Access | Rapid and quality publishing

International Journal of
Electrical and Electronics Research (IJEER)
Research Article | Volume 11, Issue 4 | Pages 1225-1239 | e-ISSN: 2347-470X

Vertebra Segmentation Based Vertebral Compression Fracture Determination from Reconstructed Spine X-Ray Images

Srinivasa Rao Gadu[1] and Chandra Sekhar Potala[2]

[1]*GITAM School of Technology, GITAM Deemed to be University; sgadu@gitam.edu*
[2]*GITAM School of Technology, GITAM Deemed to be University; cpothala@gitam.edu*

*__Correspondence:__ Srinivasa Rao Gadu; sgadu@gitam.edu

ABSTRACT- The vertebral compression fracture represents the vertebral body deformity appeared over lateral spine imageries. In order to evaluate the vertebral compression fracture (VCF), the vertebral compression ratio (VCR) has to be accurately measured. In most of the existing vertebral segmentation approaches, degraded accuracy, increased possibilities of error and time complexity are found to be the major drawbacks. Hence to conquer these issues and to enhance the overall segmentation performance, rapid automated vertebral segmentation approach is proposed for evaluating the VCR. Initially the reconstructed spine X-ray images are collected and directed over the Hybrid UDA Net architecture from this model, the features are extracted using encoder section of U-net architecture through the adoption of channel attention layer (CaL) and hybrid attention dilated Quantum convolutional layer (HaDQcL). The segmental outcomes are accomplished through the decoder section of U-Net. Based on the extracted features given as the input, exact segmentation of spinal images is attained using Twin attention mechanism called Gated-decoder attention module (GDAM). Through GDAM, the segmented spine X-ray images are obtained with effective results through the fusion of spatial and channel features in decoder attention module. The losses in the neural network are optimized using Amended pelican optimization algorithm (APoA). The diverse stages of VCF are finally analysed through VCR evaluation. The overall accuracy of 98.41%, F1 score of 96.75% and specificity of 99% is obtained by the proposed model whereas the performance is analysed using PYTHON. On comparison of proposed and existing models, the proposed model through segmentation and VCF diagnosis are highly superior.

Keywords: Deep learning; Reconstructed Spine X-rays; Vertebral compression; Spatial and Channel features; Loss Optimization; Segmentation.

ARTICLE INFORMATION

Author(s): Srinivasa Rao Gadu and Chandra Sekhar Pothala
Received: 25/04/23; **Accepted**: 01/12/23; **Published**: 26/12/2023;
e-ISSN: 2347-470X;
Paper Id: IJEER_DB_2023_04;
Citation: 10.37391/IJEER.110445
Webpage-link:
https://ijeer.forexjournal.co.in/archive/volume-11/ijeer-110445.html

Publisher's Note: FOREX Publication stays neutral with regard to Jurisdictional claims in Published maps and institutional affiliations.

1. INTRODUCTION

On account of minimized bone density and bone structure degradation, Osteoporosis is characterized as a complex clinical problem especially among the elderly people [1]. It is an age related metabolic skeletal disease whereas the pathological process is generally influenced by complex aspects like systemic hormones, life conditions, hereditary regulators and so on [2-3]. Simultaneously, the brittle fracture risk gets expanded widely through Osteoporosis and among this, vertebral fracture is considered to be one of the most difficult fracture types [4]. Patients suffering from Osteoporosis are subjected over brittle fractures and it is analysed that 50% of women and 20% of men who crossed 50 years of age gets affected more. Misdiagnosis and late analysis can be fatal over patients and approximately, 1.5 million vertebral compression fractures (VCF) are generated per year in United States.

The clinical examination of VCF is analysed through spinal images collected from patients who present back pain followed by the fracture in lumbar or thoracolumbar vertebra [5-6]. The VCF treatment differs on the basis of fracture type or kyphotic angulation evaluated over plain lateral radiographs [7]. The treatments are generally indicated if the actual vertebral height loss is estimated above 40% and kyphosis as above 30 degrees. A deformity of vertebral bodies analysed on lateral spine imaging possess to be common difficulties of Osteoporosis that frequently leads to spinal deformity, back pain, functional inability and every tends to death [8-9]. Hence, they are considered as one of the most threatening diseases which maximizes the economic society burden [10]. The major clinical perspective of VCF is compression, collapsing, vertebral body wedging and generally exposing lumbago.

Medical images captured in the form of X-rays, CT and MRI images allows VCF diagnosis [11]. As spinal X-ray images consists of lateral and anteroposterior exposures of vertebrae, it acts as a basic diagnostic modality in case of VCFs as it promotes imaging modality accessibility speed over clinical practices [12-13]. Prominent determination of VCFs is often considered as a conservative treatment failure [14]. Hence an efficient, reproducible and reliable radiographic evaluations are required for better clinical decision making. There are diverse radiographic evaluation parameters including anterior vertebral body compression percentage, Cobb angle and vertebral compression ratio (VCR). The typical index for VCF diagnosis

FOREX Publication
Open Access | Rapid and quality publishing
International Journal of Electrical and Electronics Research (IJEER)
Research Article | Volume 11, Issue 4 | Pages 1225-1239 | e-ISSN: 2347-470X

is VCR that represents the ratio of normal or abnormal anterior vertebral height (AVH). The AVH estimation acts as a standard spinal disorder diagnosis like VCF or scoliosis.

Across multiple studies, AI (Artificial Intelligence) has become popular in medical imaging applications that demonstrated exceptional performance and positive outcomes [15-16]. Recently, the deep learning (DL) strategy has obtained greater attention towards automatic capability in critical feature extraction [17-18]. In specific, the process becomes quite easier to analyse the huge complex data. The DL models like CNN (Convolutional Neural Network) [19] and LSTM (Long Short-Term Memory) [20] are employed in multiple research studies which possessed a generalized performance and efficient processing of medical images. To conquer the short comings of manual VCR estimation, an efficient algorithm that segments the vertebral bodies and evaluates VCR automatically has been proposed to minimalize the observer variability and to promote better reliability and reproducibility.

The VCF influences most of the individuals across worldwide and they are most commonly occurring among elderly people. The VCFs have the tendency to generate significant morbidity, disability and incapacitating back pain for a long period of time. For an efficient detection of VCF, appropriate segmentation of spinal x-ray images has to be carried. As mostly, the observations are done manually by the clinicians, there are lot of chances in measurement value variations. Also, the technical quality of radiograph and succeeding interpretation capability of clinicians can be influenced. The likelihood of mis-diagnosis, delayed observations and inter observer variability gets maximized through manual evaluation of compression ratio. The VCR detection standard is found to be hard to analyse because deformity evaluation varies on account of scan portions, way of estimation and vertebral body deformity after abnormal conditions.

Recently, considerable number of researches has been carried using DL methodologies to attain improved performance compared to machine learning approaches in spinal disease diagnosis assistance. Even though, more researches are carried for VCF diagnosis, exact segmentation of vertebra cannot be attained through the estimation of in-vertebral disc height and vertebral body height. It is highly difficult to notice the minute radiography variations. Most of the system models are costly, less reliability and reproducibility. Because of image size and pixel spacing variations among patients, there are more chances for error occurrence. Hence to overcome the complexities, an automated VCF identification system with VCR evaluation is perceived to promote improved outcomes through effective vertebral segmentation.

A novel technique called Hybrid UDA Net based DL framework is proposed for the precise segmentation of reconstructed spinal X-rays. Some of the prospective contributions for promoting the overall accuracy are described as follows.

- To introduce a novel Hybrid UDA Net for extracting valuable features and to segment the vertebral images using reconstructed spine X-rays.
- To extract the significant features using CaL and HaDQcL through the integration of attention mechanisms and quantum layers whereas the segmentation is carried through twin attention mechanism.
- To optimize the loss functions using Amended pelican optimization algorithm and to analyse diverse stages of VCF through VCR evaluation.
- To analyse the overall performance of proposed VCF diagnosis model by estimating certain metrics like accuracy, sensitivity and specificity to prove its efficiency by comparing the outcomes with existing methodologies.

Rest of the details are organized into diverse sections which are described as follows. *Section 2* signifies the related existing research works done by various authors in vertebral segmentation. *Section 3* labels the work flow of proposed methodology carried through different steps for feature extraction, segmentation and VCF evaluation. The outcomes and performance analysis of vertebral segmentation based on DL model is presented in *Section 4*. *Section 5* renders the conclusion of proposed work pursued by future scope with references.

2. RELATED WORKS

Relying upon vertebral segmentation, most of the researchers have proposed diverse methods to yield accurate results. The works analyzed through some of the substantial segmentation techniques are surveyed as follows.

The ability of CNN was evaluated in Monchka et al. [21] for generalization between General Electric (GE) dual energy and GE single energy vertebral fracture assessment scan modes. The imageries attained from Manitoba Bone Mineral Density Program was exported in both dual and single energy modes. The presence and absence of fracture were classified effectively through the adoption of modified algorithm-based qualitative (mABQ) technique. Better performance was analysed in training the CNN simultaneously over both Single and dual energy. The single energy evaluation dataset has attained 90.6% of accuracy and dual energy evaluation dataset has obtained 92.3% of accuracy.

Kong et al. [22] presented CNN based prediction model called DeepSurv for determining the vertebral fractures. The proposed study included 1595 participants of 50 to 75 years old with at least two lumbosacral radiographs without existing fractures. Here the vertebral fractures were analysed based on the positive and negative cases. The performance was analysed on the basis of concordance index (C-index) which are then compared between DeepSurv, Cox proportional hazard (CoxPH) approaches and Fracture Risk Assessment Tool (FRAX). The C-index of CoxPH falls to be 0.594, FRAX had attained 0.547 and DeepSurv had attained 0.612 whereas DeepSurv model showed better performance.

FOREX Publication
Open Access | Rapid and quality publishing
International Journal of Electrical and Electronics Research (IJEER)
Research Article | Volume 11, Issue 4 | Pages 1225-1239 | e-ISSN: 2347-470X

The CT radiography and DL approaches were integrated for predicting osteoporotic CT images. In the research work proposed by Hu et al. [23], the CNN model was utilized for classification and network weights were updated through Adam optimizer with the integration of exponentially weighted moving average gradients methods and momentum. The model accuracy of 83.9% was obtained in subsequent fracture prediction and 88.3% was obtained in case of receiver operating characteristic (ROC)–area under curve (AUC) over the consideration of whole testing dataset. The presented model can able to predict osteoporotic VCF using CT images in an accurate and unbiased manner.

Iyer et al. [24] presented three-dimensional localization of lumbar spine and thoracic portions through the adoption of deep reinforcement and imitation learning. Around the coronal entre, the localised portions are then separated into two dimensional sagittal slices. All slices are then separated into patches and in that CNN is trained to analyse the compression fractures of spinal region. After the process of localization, the accuracy of 80%, specificity of 80.73% and sensitivity of 79.87% were attained in VCF detection from fivefold cross validation. The outcomes of VCF detection were analysed in case of 3 layered and 6 layered CNN. Effective localization performance can be attained but the training ability was very less.

The performance of vertebral compression measurement and vertebral body segmentation model were demonstrated by Seo et al. [25] with VCF diagnosis using X-ray images. The residual recurrent U net model was employed for segmenting vertebral body. The average accuracy of 98.7%, average dice similarity coefficient of 92.3% and sensitivity of 93.4% were obtained. Linear regression and multi-scale residual dilated blocks were employed for detecting VCF whereas the mean absolute error of 2.637 was attained. Error rates can be effectively minimized but degraded results were attained due to inefficient pre-processing of X-ray images. *Table 1* shows the analysis of existing VCF detection-based models.

Table 1: Analysis of VCF detection-based models with its merits and demerits

Author name and Reference	Technique used	Objective	Merits	Demerits	Performance (%)
Monchka et al. [21]	mABQ	To assess the capability of CNN to generalize GE dual and single energy vertebral fracture assessment scan modes.	- Better generalization performance. - Highly feasible over manufacturer-independent models	-Complex to handle huge datasets -Consumes more time.	Ac curacy- 90.6 (single energy evaluation dataset) Accuracy- 92.3 (Dual energy evaluation dataset)
Kong *et al.* [22]	DeepSurv	To develop a fracture prediction model using DL with longitudinal data to promote better efficiency.	Prediction of osteoporotic fracture from spine radiographs are efficient.	The model performance was degraded due to the small test set selection bias.	C-index-0.612
Hu *et al.* [23]	CNN with Adam optimizer	To generate DL based model for predicting successive osteoporotic VCF using CT images.	-Tends to be a better application prospect -Promote effective	Higher onset time in handling data	Accuracy- 83.9, ROC-AUC- 88.3
Iyer *et al.* [24]	CNN with markov decision process and deep Q learning.	To accomplish 3D localization of lumbar spine and thoracic regions for effective VCF detection.	-Better localization performance - Cost effective	-Training ability was less -Increased computational complexity	Accuracy-80%, Specificity-80.73% and Sensitivity-79.87%
Seo *et al.* [25]	Residual recurrent U net model and Linear regression	To perform vertebral body segmentation and vertebral compression evaluation using X-ray images.	Effective minimization of error rates	Degraded VCF detection outcomes due to quality less images.	Accuracy-98.7, Average dice similarity coefficient-92.3, sensitivity-93.4 and MAE- 2.637

FOREX Publication
Open Access | Rapid and quality publishing
International Journal of Electrical and Electronics Research (IJEER)
Research Article | Volume 11, Issue 4 | Pages 1225-1239 | e-ISSN: 2347-470X

When examining the related surveys over existing approaches in accordance to vertebral segmentation, various complexities that adversely influence the segmentation performance are emerging. The limitations include inaccurate vertebral segmentation due to non-effective consideration of relevant features. Because of increased feature complexity, less ability is seen in handling training data and high processing time is required for evaluating the performance. The outcomes of VCF evaluation are degraded because of processing low quality images. Due to the existence of these difficulties, performance of vertebral segmentation and VCF evaluation using vertebral images are affected. To overcome the complexities of existing approaches and to enhance the segmentation accuracy, a novel DL method is proposed in this research article to obtain efficient outcomes.

3. PROPOSED METHODOLOGY

The accurate vertebral segmentation could assist in identifying exact compression fracture and progress evaluation. Automatic vertebra segmentation is highly desirable as manual segmentation tends to be time consuming and cumbersome. Automatic process can support the clinicians to assess and minimize misdiagnosis generated by human error. As the requirement of exact VCF diagnosis is essential in the recent days, an accurate segmentation of spinal images is essential to measure VCR. For rapid accurate segmentation with minimized time consumption and to generate effective outcomes, DL based approach is employed. In this research, an automated DL based vertebral segmentation and VCF stage analysis through VCR estimation using reconstructed spine X-rays. *Figure 1* demonstrates the overall architecture of proposed research model 3.1 Subsection.

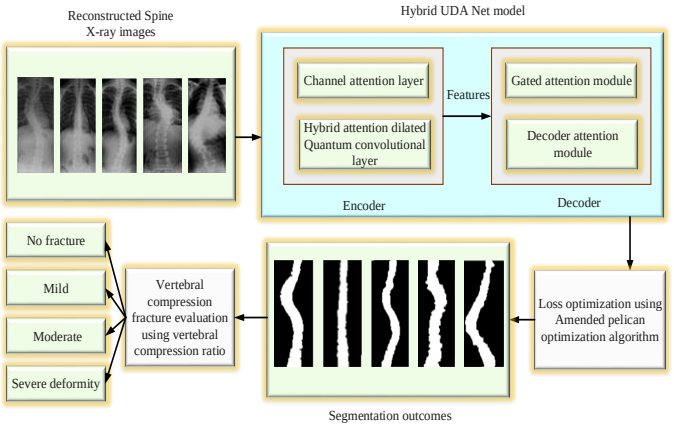

Figure 1: Block architecture of overall proposed model

The diverse steps involved in VCF diagnosis are data acquisition, vertebral segmentation and VCF diagnosis. After the collection of data from reconstructed spine X-rays, the features are extracted from the encoder section of U-net using CaL and HaDQcL. Based on the extracted features given as the input, exact segmentation of spinal images is attained using Twin attention mechanism called GDAM. The losses in the neural network are optimized using APoA whereas the diverse stages of VCF are finally analysed through VCR evaluation.

The proposed Hybrid UDA Net architecture is comprised of encoding and decoding branch whereas the encoding branch acts as a feature extractor and the decoder branch generates the segmentation outcomes.

3.1 Hybrid UDA Net Architecture

The encoding section utilizes the fundamental residual block with two successive convolution layers whereas each convolution is pursued by a batch normalization and nonlinear ReLU layer. Each residual block is pursued by a 2×2 max-pooling process. The HaDQcL present in the final layer generates the summarized feature outcome as the output of encoder. The outcome of summarized features are merged with the decoder section insisting the DA network architecture. The exact segmentation of vertebral portions are carried through GDAM whereas the gated attention module is employed inside the skip connection strategy to minimize the semantic gap between encoder and decoder. The decoder attention module concentrates on spatial and channel features which are then merged through fused attention mechanism to obtain refined segmentation outcomes. In Hybrid UDA Net architecture, huge batch normalization layers are used as it enhances the stability, training process speed and standardize the inputs of network layers. The block wise explanation of Hybrid UDA Net architecture are clearly described in the following sub-sections with appropriate figures. *Figure 2* demonstrates the architecture of proposed Hybrid UDA Net research model.

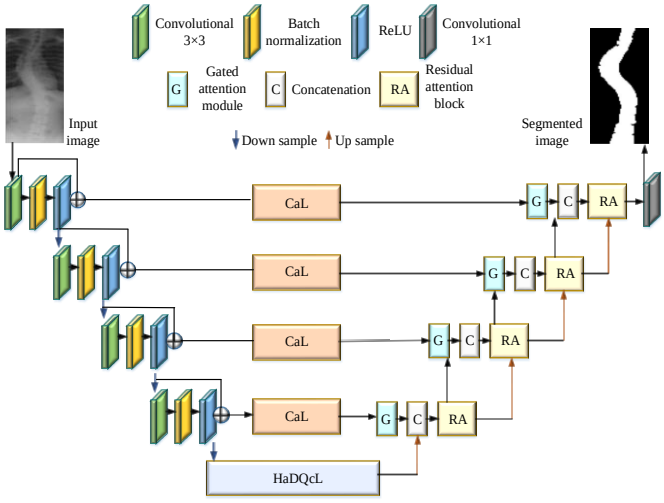

Figure 2: Hybrid UDA Net architecture

3.1.1 Channel Attention Layer

Every channel relates over a specified semantic response whereas diverse channels possess specific assistances to obtain significant feature information. The main objective of CaL is to enhance the representation capability of network by modelling every channel dependency. The features can be altered channel by channel and so the network can choose the strengthened features owning significant information. By this, the unwanted features that contain useless information are supressed effectively. Through the addition of CaL for every skip connection, the non-significant redundant information can be eliminated. Through channel map interdependence leveraging,

FOREX Publication
Open Access | Rapid and quality publishing
International Journal of Electrical and Electronics Research (IJEER)
Research Article | Volume 11, Issue 4 | Pages 1225-1239 | e-ISSN: 2347-470X

the suitable feature representations can be refined. The channel attention (CA) block is employed for simulating the channel interdependence. The structure of CA block is provided in *figure 3*.

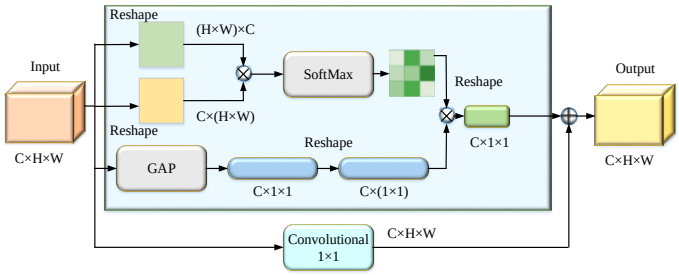

Figure 3: Structure of CA block

Initially, the input feature map$F \in R^{C\times H\times W}$is reshaped into$U \in R^{C\times(H\times W)}andV \in R^{(H\times W)\times C}$ correspondingly. The product of matrix$U$and$V$is divided by$\sqrt{D}$factor. Finally, the CA map$W \in R^{C\times C}$is obtained through the application of softmax layer.

$$z_{ab} = Soft\,max\left(\frac{Func(F_a,F_b}{\sqrt{D}}\right) \quad (1)$$

From the above expression, the b^{th} channel effect over a^{th}channel is formulated as z_{ab}, the relation between$b$and every$a$are estimated by the function $Func$. The global average pooling (GAP) layer is employed to obtain the channel statistics of original feature map$V \in R^{C\times H\times W}$channel reduced into global spatial data. The GAP compresses global information and attains an attention vector for minimizing the feature dimensionality and to extract high level semantic information. Through the process of vector encoding, the important features can be conserved. The matrix multiplication is executed between W and V which are transformed over $R^{C\times 1\times 1}$. The obtained outcome is multiplied with the proportional parameterδwhereas$F$is used after 1×1 convolution for summation to attain the final outcome$O \in R^{C\times H\times W}$.

$$GAP(F_m) = \frac{1}{H\times W}\sum_{a=1}^{H}\sum_{b=1}^{W} F_m(a,b) \quad (2)$$

From the above expression, global average pooling is represented as$GAP$and $m = 1,2,\ldots.c, F = [f_1, f_2, \ldots. f_c]$

$$O_b = \delta\sum_{a=1}^{C}(z_{ab}.GAP(F_m)) + W_0F_b + B_0 \quad (3)$$

The parameterδinitiates from 0, B_0denotes the bias and the weights W_0 are learnt using training that refers to 1×1 convolution weight. The above equation indicates the final outcome of weighted sum between convolutional feature maps and features that emerge from self-attention with GAP. The spatial information of all suitable locations are utilized for channel correlation modelling and channel relation explore through global pooling.

3.1.2 Hybrid Attention Dilated Quantum Convolution Layer

The HaDQcL is comprised of three bottleneck dilated quantum convolution modules with diverse dilated rates and one CaL module. The bottleneck dilated modules are comprised of 1×1, 3×3 and 1×1 quantum convolutional layers with a residual connection. Through this module, the arbitrary expansion of receptive field can be attained without additional parameters. The structure of HaDQcL block is illustrated in *figure 4*.

The quantum convolutional layer applies the pooling and convolution layer over quantum systems. The convolution circuit determines the hidden state through the application of numerous qubits. The pooling circuit minimizes the quantum system size and the process is repeated. On considering the 2D image, the dilated convolution can be signified as,

$$g(b) = \sum_{m=1}^{m} h(b + d.m)f(m) \quad (4)$$

From the above expression, the input signal is signified as and the output signal as. The filter with convolutional kernel size is indicated as and dilated convolution rate is defined as whereas is the standard convolution.

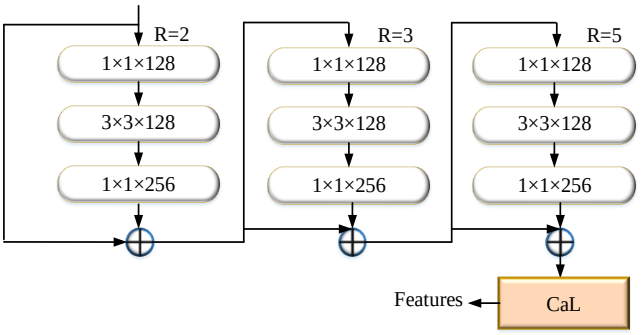

Figure 4: Structure of HaDQcL block

In accordance to the above equation, the convolution kernel is denoted as, resultant dilated filter with size whereas. The reason for utilizing dilated convolution is to tackle different object size simultaneously. The dilated convolutional cascade rate is modelled to be 2, 3 and 5 to satisfy the below expression.

$$D\,max_b = Max[d_b, D\,max_{b+1} - 2d_b, D\,max_{b+1} - 2(D\,max_{b+1} - d_b)] \quad (5)$$

The dilated rate of $b$layer is denoted as$d_b$and maximum dilated rate in the$b$layer is represented as$D\,max_b$. On considering the convolutional kernel size as $m \times m$, the target is$D\,max_2 \leq m$. On cascading numerous bottlenecks dilated modules with diverse dilated rates, the multi Zscaler context information can be extracted fully whereas the number of parameters is effectively minimized. The residual connection is added for every bottleneck dilated module that are conductive over network optimization. The CA block is employed for non-linear information fusion of every channel. The non-linear function is applied for denoting the context information relation of diverse channels and the weights are allotted over multi-scale context information for facilitating crucial feature extraction.

3.1.3 Twin attention mechanism

In the decoder section of Hybrid UDA Net architecture, the twin attention mechanisms are employed to obtain better segmentation outcomes. The gated attention module is

FOREX Publication
Open Access | Rapid and quality publishing
International Journal of Electrical and Electronics Research (IJEER)
Research Article | Volume 11, Issue 4 | Pages 1225-1239 | e-ISSN: 2347-470X

employed inside the skip connection strategy for reducing the semantic gap between encoder and decoder. The spatial and channel features are merged through fused attention mechanism in the decoder attention module for effective segmentation outcomes. The twin attention mechanism called GDAM is introduced in the decoder section for further suppressing of false positives. The gated attention module is utilized for refining the extracted features and to minimize the semantic gap by merging high as well as low level feature maps. For refining the feature representations and suppress the noise after up sampling, the decoder attention module is presented.

3.1.3.1 Gated attention module

The concatenation of features from the encoder to decoder is the fundamental structure in U-Net whereas the integration of higher resolution features, up sampled features in the encoder and decoder enables the segmentation targets. The gated attention module is subjected to concatenate for minimizing the semantic gap between encoder and decoder. Both the spatial and channel attention can be enabled through this module. The detailed architecture of gated attention module is depicted in *figure 5*.

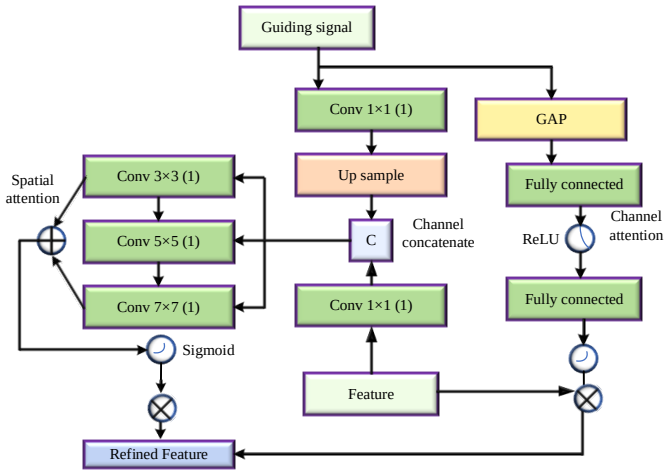

Figure 5: Structure of gated attention module

Two feature maps are directed over the attention module whereas the guiding signal is referred as the feature map from decoder. The guiding signal is represented as $P \in R^{C_p \times H_p \times W_p}$ and the feature is represented as $F \in R^{C_f \times H_f \times W_f}$. More semantic information is there in P compared to F. The GAP operation pursued by multi-layer perceptron (MLP) is utilized to generate the channel attention map $CA_m(F) \in R^{C_f \times 1 \times 1}$. The channel attention can be formulated as follows.

$$CA_m(F) = \mu(MLP(GAP(P))) = W_{C_f}(RELU(W_{C_p/r}(GAP(P))) \quad (6)$$

The sigmoid function is represented as μ, reduce ratio is expressed as r, $W_{C_p} \in R^{C_p/r \times C_p}$ and $W_{C_f} \in R^{C_f \times C_p/r}$. The spatial attention is guided both by the input feature and guiding signal. To compress the channel dimension of P and F, convolution operation with one filter is employed. The integration of convolution operation with diverse kernel size is employed to generate spatial attentions $SP_m(F) \in R^{1 \times H_f \times W_f}$. The spatial attention can be formulated as follows.

$$SP_m(F) = \mu(f_{3\times3}(|F_r, P_r|)) + (f_{5\times5}(|F_r, P_r|)) + (f_{7\times7}(|F_r, P_r|)) \quad (7)$$

From the above expression, $F_r = f^r_{1\times1}(F)$ and $P_r = US(f^r_{1\times1}(P))$. The convolution operation with respective kernel size is denoted as $f_{3\times3}$, $f_{5\times5}$ and $f_{7\times7}$. The sigmoid function is denoted as and μ is employed to squeeze the channel dimension. In order to generate the fused attention, element wise multiplication is employed.

$$K(F) = F * SP_m(F) * CA_m(F) \quad (8)$$

The element wise multiplication is denoted by the symbol $*$.

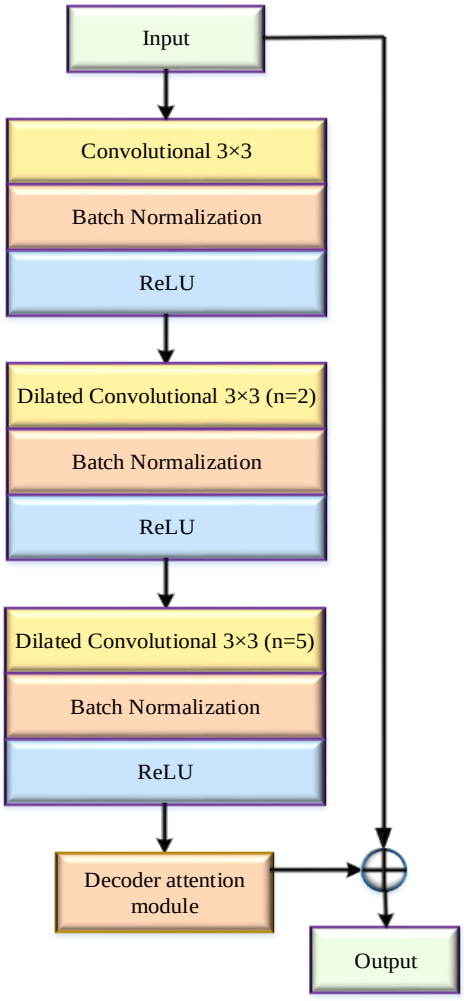

Figure 6: Residual attention block architecture

The multiscale patterns of unsampled feature maps are captured through dilated convolutions. The RA block comprises a pile of dilated convolutions with 3 kernel size. The RA block is pursued by the decoder attention module. The initial receptive field is assumed to be 1×1 and the corresponding dilated convolution kernel size can be estimated as follows.

$$S = s + (s-1)(u-1) \quad (9)$$

FOREX Publication
Open Access | Rapid and quality publishing
International Journal of Electrical and Electronics Research (IJEER)
Research Article | Volume 11, Issue 4 | Pages 1225-1239 | e-ISSN: 2347-470X

The corresponding kernel size can be represented as S, the actual kernel size is denoted as S and the dilation rate is represented as u. The dilation rates are set to be (1, 2, 5) that obtains huge receptive field. Because of piled dilated convolutions, the huge receptive field of 17×17 is obtained that captures the global information. Multiscale information of feature maps can be captured by using diverse dilation rates which is highly useful for accurate segmentation. The residual connections are utilized in RA block to overcome gradient vanishing problems. In order to generate fused attention maps and to refine the up sampled features, the dilated convolutions are pursued by a decoder attention module. The outcome of RA block can be expressed as follows.

$$O = L + Dec_{AM}(H_{DC}(L)) \quad (10)$$

From the above expression, Lindicates the input feature maps, O signifies the output feature maps, Dec_{AM} represents the decoder attention module and H_{DC} indicates the hybrid dilated convolutions.

3.1.3.2.1 Decoder Attention Module

In the process of effective segmentation, the visual descriptions with high resolution have to be up sampled in the encoder. The decoder attention module is employed to solve the issue of non-significant information to the up-sampling process. The architecture of decoder attention module is depicted in *figure 7*.

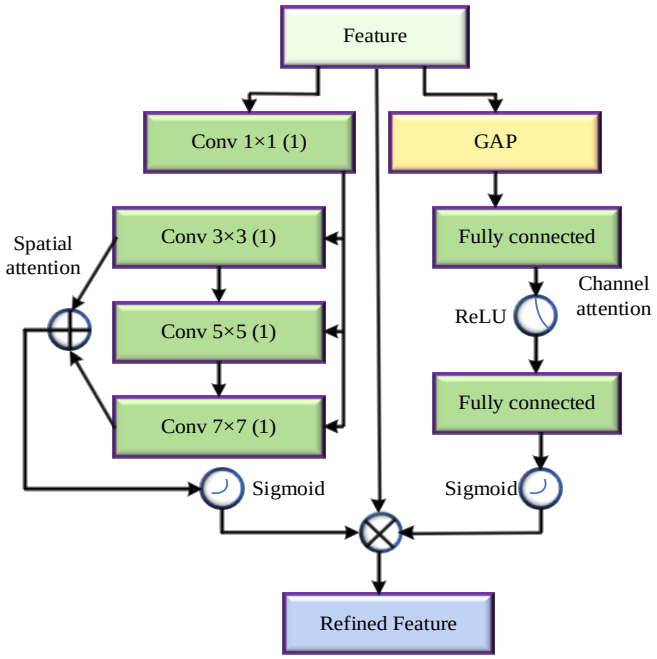

Figure 7: Decoder attention module

In order to refine the post up sampling feature maps, a merged attention approach is utilized in both spatial and channel dimensions. The presented module considers one input and simple compared to the gated attention whereas the channel and spatial attention execution is quite same. The channel attention is denoted as $CA_m(F) \in R^{C\times1\times1}$, spatial attention is represented as $SP_m(F) \in R^{1\times H\times W}$and fused attention is defined as $K(F)$. The computation of decoder attention module can be evaluated as follows.

$$CA_m(F) = \mu(MLP(GAP(P))) = W_1(RELU(W_0(GAP(P)))) \quad (11)$$

The sigmoid function is represented as μ, the reduce ratio is indicated as r , $W_0 \in R^{C/r\times C}$ and $W_1 \in R^{C\times C/r}$. The spatial attention can be computed as,

$$SP_m(F) = \mu(f_{3\times3}(f^r_{1\times1}(F)) + f_{5\times5}(f^r_{5\times5}(F)) + f_{7\times7}(f^r_{1\times1}(F)) \quad (12)$$

The convolution process with respective kernel size is indicated as$f_{3\times3}$, $f_{5\times5}$ and $f_{7\times7}$ whereas $f^r_{1\times1}$ is utilized to compress the channel dimension.

$$K(F) = F * SP_m(F) * CA_m(F) \quad (13)$$

The element wise multiplication is denoted by the symbol $*$. The losses generated in the neural network are optimized using APoA approach. Initially, the population are initialized randomly deliberating to the upper and lower bound based on the below expression.

$$R_{j,k} = Low_k + Random(Upp_k - Low_k), j = 1,2,3,\ldots..,P, k = 1,2,3,\ldots..,Q \quad (14)$$

where, Q indicates the problem variables, $R_{j,k}$ symbolises the value of k^{th} variable quantified through j^{th} candidate solution, P specifies the number of population members, Low_k defines the k^{th} lower bound, Upp_k signifies the k^{th} upper bound, and $Random$ represents the random number of range [0,1].

Movement towards prey

In this phase, the location of prey can be identified and then the pelicans rush towards it from a high altitude. The exploration capability of the pelican can be maximized through the random distribution of the prey. The update of pelican's position at every iteration can be signified as,

$$R^{t+1}_{j,k} = \begin{cases} R^t{}_{j,k} + Random(s^t{}_k - \delta.R^t{}_{j,k}), P_s < P_j; \\ R^t{}_{j,k} + Random(R^t{}_{j,k} - s^t{}_k), else, \end{cases} \quad (15)$$

where, t indicates the present iteration number and$s^t{}_k$ means the prey location in k^{th} dimension. $R^t_{j,k}$ specifies the new status of j^{th} pelican in k^{th} dimension depending on first stage, P_s characterizes the value of objective function with minimized loss function and δ specifies the random number equal to 1 or 2.

Winging towards water surface

Once the pelicans attain the water surface, the wings are spread over the water surface to move the fish in a upward direction. After that, the prey is collected in the throat pouch. The hunting behaviour of pelicans can be mathematically expressed a

$$R^{t+1}_{j,k} = R^t{}_{j,k} + \lambda\left(1 - \frac{t}{T}\right)(2.Random - 1).R^t{}_{j,k} \quad (16)$$

From the above expression, the new status of j^{th} pelican in j^{th} dimension based on exploitation is denoted as $R^{t+1}_{j,k}$, and the constant λ is equal to 0.2 . $\lambda\left(1 - {}^t/_T\right)$ indicates the neighbourhood radius, w means the iteration counter and W

FOREX Publication
Open Access | Rapid and quality publishing
International Journal of Electrical and Electronics Research (IJEER)
Research Article | Volume 11, Issue 4 | Pages 1225-1239 | e-ISSN: 2347-470X

represents the maximum iteration. In order to enhance the loss optimization efficiency, the APoA strategy is employed. During the initialization strategy, tent chaotic map is employed to swap random generation and the *equation (15)* can be reframed as,

$$R_{j,k} = Low_k + TC(Upp_k - Low_k), j = 1,2,3,\ldots\ldots,P, k = 1,2,3,\ldots\ldots,Q \quad (17)$$

$$TC^{t+1} = \begin{Bmatrix} \frac{TC^t}{m}, Tent^t \in (0,m) \\ \frac{1-TC^t}{1-m}, Tent^t \in (m,1) \end{Bmatrix} \quad (18)$$

The pelican position is initialized using tent chaotic map (TC) that helps to enhance the global searching performance. In movement towards prey stage, dynamic weight factor$\eta$is used to update the pelican position. At this stage, the pelican is able to continue a better global search. At the iteration end, ηminimizes adaptively whereas the pelican performs a better local search while maximizing the convergence speed. The equation (15) can be reframed as follows.

$$R_{j,k}^{t+1} = \begin{cases} \eta = \frac{e^{2(1-t/T)} - e^{-2(1-t/T)}}{e^{2(1-t/T)} + e^{-2(1-t/T)}} \\ R^t{}_{j,k} + Random(s^t{}_k - \delta . R^t{}_{j,k}), P_s < P_j; \\ R^t{}_{j,k} + Random(R^t{}_{j,k} - s^t{}_k), else, \end{cases} \quad (19)$$

The APoA strategy is highly significant in optimizing the loss function emerged in the segmentation network model. On performing several iterations using APoA, the loss functions can be optimized better and so the error rate can be extensively minimized. Finally, from the Hybrid UDA Net architecture, effective segmentation outcomes can be obtained.

3.2 Evaluation of Vertebral Compression Ratio

The ratio of abnormal to normal height of vertebral body is termed as VCR. It is evaluated through the ratio of anterior vertebral height to the adjacent anterior vertebral height corresponding to the vertebral body. It acts as a significant indicator to diagnose VCF and the formula to estimate VCR is given as follows.

$$VCR = (1 - \left(\frac{V_2}{(V_1+V_3)\times\frac{1}{2}}\right) \times 100)\% \quad (20)$$

Using the above formula, the diverse stages of VCF can be evaluated based on the range value. The extent of VCR estimation identifies the below stages effectively.

- No fracture identified from the segmented image if the VCR range is between 0-20%.
- Mild fracture identified from the segmented image if the VCR range is between 20-25%.
- Moderate fracture identified from segmented image if the VCR range is between 25-40%.

Severe deformity fracture identified from the segmented image if the VCR range is greater than 40%.

3.3 Evaluation of Cobb Angle

One of the most widely used evaluations for quantifying spine curvature is Cobb angle. The curvature of the Cobb approach is signified as the angle between upper border of upper vertebra and lower border of lower vertebra. The spine curvature can be assessed using the below given formula.

$$\theta = Max\left\{\left|tan^{-1}\left(\frac{p_a - p_b}{1+p_a \times p_b}\right)\right|\right\} \quad (21)$$

From the above expression, $(a,b) \in \{(u,v)|u \in N, v \in N, v - u \geq 2 and v \leq N\}$. Here, u indicates the upper vertebra and v indicates the lower vertebra with at least one vertebrae interval from upper vertebra $u.p_a$ represents the slope of upper border of upper vertebra and p_b indicates the slope of lower border of lower vertebra. N denotes the number of counted vertebra samples and through the Cobb angle measurement, diverse stages like normal, mild, moderate and severe spine curvature. *Table 2* describes the Cobb angle range in determining the stages of spine curvature.

Table 2: Cobb angle analysis

Cobb angle	Stage of spine curvature
$0° - 10°$	Normal
$10° - 20°$	Mild fracture
$20° - 40°$	Moderate fracture
$> 40°$	Severe fracture

Through the implementation of this research work, the diverse stages of reconstructed spine X-ray images can be effectively analysed through VCF and Cobb angle detection. The optimal outcomes can be attained because of highly precise segmented image outcomes gained through the novel Hybrid UDA Net architecture model.

4. RESULTS AND DISCUSSION

The proposed Hybrid UDA Net architecture is inspected with extraction of features, segmentation and VCF evaluation. Initially, the reconstructed spine X-ray images are fed into the Hybrid UDA Net model that performs feature extraction and segmentation process. For effective segmentation outcomes, the losses are optimized whereas diverse stages of VCF are determined through VCR evaluation. The experimental outcomes of proposed model are represented in this section. The performances of proposed model are evaluated through the implementation using PYTHON. To estimate the proposed segmentation performance, numerous existing models are compared. The dataset details, description of performance metrics with its corresponding mathematical formulation, performance analysis and comparison are established in the following sub-sections.

4.1 Dataset Details

The dataset generated by the London Health Sciences Center professionals and the dataset comprises of 609 anterior-posterior spinal x-ray images. The dataset has been collected from http://spineweb.digitalimaginggroup.ca [26]. The collected images are reconstructed and then used as the input in the proposed research work. The reconstructed spinal X-ray images are used for effective vertebral segmentation and VCF evaluation. In the proposed research work of vertebral

FOREX Publication
Open Access | Rapid and quality publishing
International Journal of Electrical and Electronics Research (IJEER)
Research Article | Volume 11, Issue 4 | Pages 1225-1239 | e-ISSN: 2347-470X

segmentation, 80% of data is used for training and 20% for testing.

4.2 Metrics used for Performance Analysis

The proposed performance of vertebral segmentation can be measured through the consideration of diverse metrics including Accuracy, Sensitivity, Precision, Specificity, F1 score, root mean square error (RMSE) and dice similarity coefficient. The description of considered metrics are provided with its mathematical formulations for analysing the proposed performance in *table 3*.

Table 3: Performance metrics and its Formulation

Performance Metrics	Description	Mathematical formulation
Accuracy	The summation of true positive and negative to the overall summation of true and false metrics is termed as accuracy.	$A = \frac{K+L}{K+L+M+N}$ K -True positive, L -True negative, M -False positive, N -False negative.
Specificity	The number of negative results to the entire samples which are truly negative is termed as specificity.	$SPE = \frac{L}{L+M}$
Dice similarity	The dice similarity coefficient is the statistical tool used to evaluate the similarity between two sets of data.	$DS = \frac{2K}{(2K+M+N)}$
F1 score	The combination of precision or positive predictive rate and recall or negative predictive rate to a single value is termed as F1 score.	$F1S = 2\frac{PPV \times TPR}{PPV + TPR}$
Recall	The segmentation outcomes are considered to be highly sensitive if the data generates positive cases.	$SEN = \frac{K}{K+N}$
Precision	The section of significant information from the gathered data improves the precision performance.	$P = \frac{K}{K+M}$
RMSE	RMSE indicates the standard deviation of segmentation errors.	$RMSE = \sqrt{\frac{\sum_{F=1}^{N}(a_i - \hat{a}_i)^2}{N}}$ $\hat{a}_i$ - predicted observations, a_i-actual observations, N - Total samples

4.3 Baseline Model Comparison

The performances of proposed Hybrid UDA Net model are compared with the existing approaches whereas the results are analysed in terms of diverse performance metrics. The detailed description of performance analysis with respect to each metrics are presented clearly in the form of graphical representations. The system configuration details and hyper parameter settings of the proposed work are provided in *table 4* and *table 5*.

Table 4: System configuration details

Sl. No	Parameters	Configuration
1	Pen and touch	No pen or touch input is available for the display
2	System type	64-bit operating system, x64 based processor
3	Installed RAM	12.0 GB
4	Processor	Intel(R) Core (TM) i5-3570 CPU @ 3.40GHz

Table 5: Proposed hyper parameter settings

Sl. No	Hyper-parameters	Proposed model
1.	Batch size	128
2.	Initial learning rate	0.0001
3.	Maximum epoch size	300
4.	Activation function	Sigmoid
5.	Total number of layers	60
6.	Maximum iteration	100
7.	Dropout rate	0.1

The existing models like Otsu thresholding (OT), Fuzzy C-means clustering (FCM), Convolutional neural network (CNN) and SEGNET are compared with the proposed model. The performances of proposed model are analysed by considering the metrics like accuracy, specificity, dice similarity coefficient and F-measure. *Figure 8* depicts the proposed and existing performance comparison outcomes with respect to accuracy, specificity and F-measure.

FOREX Publication
Open Access | Rapid and quality publishing
International Journal of Electrical and Electronics Research (IJEER)
Research Article | Volume 11, Issue 4 | Pages 1225-1239 | e-ISSN: 2347-470X

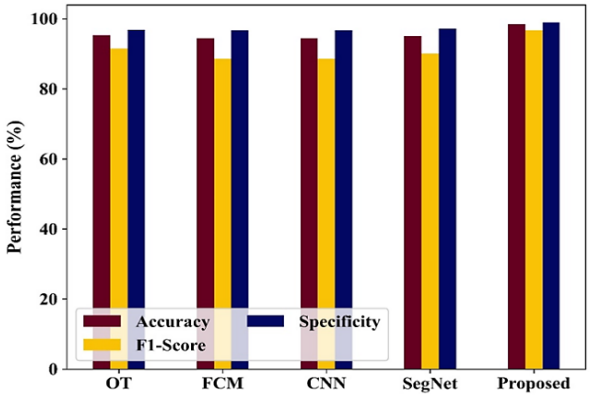

Figure 8: Performance Comparison

The effectiveness of vertebral segmentation can be analysed through finest extraction of features and segmentation using Hybrid UDA Net architecture. From the figure, it can be clearly stated that the proposed model obtained higher rates of accuracy, F1 score and specificity. The accuracy of 98.41% is obtained by the proposed model whereas the existing models like OT has attained 95.31%, FCM as 94.40%, CNN as 94.40% and SEGNET as 95.12% of accuracy. The specificity rate of proposed model is obtained to be 99% whereas OT has attained 96.83%, FCM as 96.73%, CNN as 96.73% and SEGNET as 97.15% respectively. The F1-score of proposed model is obtained to be 96.75% whereas OT has attained 91.47%, FCM as 88.57%, CNN as 88.57% and SEGNET as 90.04% respectively. Due to the effective utilization of features, proposed model performances are comparatively better. The existing performances are degraded because of less capability in learning significant features. The existing models has obtained inferior performance than the proposed model due to certain drawbacks like less robustness, increased training time and larger accumulation of features. *Figure 9 (a)-(b)* indicates the performance of Precision-Recall (PR) curve and region operating characteristic (ROC) curve.

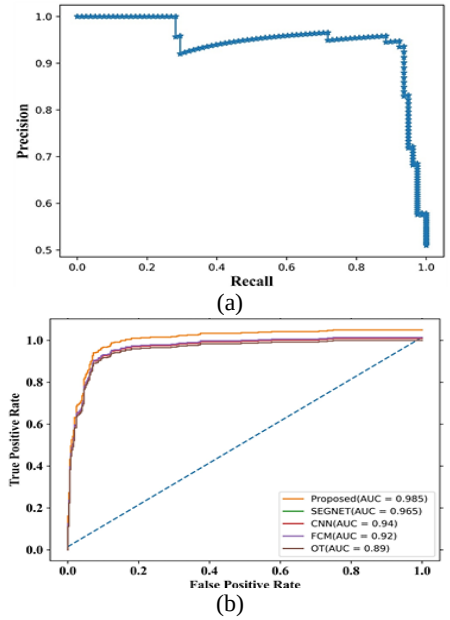

Figure 9: Performance analysis (a) PR curve (b) ROC curve

The precision-recall curve usually tends to explore the trade-off between precision and recall. Also, it is used to measure the segmentation effectiveness. The precision-recall curve is assessed to analyse the heavily imbalanced cases. The precision of 96.75% and recall of 96.75% is obtained by the proposed model. The AUC analysis of proposed model is analysed using ROC curve and it demonstrates better capability to distinguish the target classes. The ROC curve is plotted between FPR and TPR whereas the ability in vertebral segmentation is enhanced based on respective input parameters. The optimum cut-off displays the maximum sensitivity with minimum specificity. The ROC curves are frequently inspected to expose the trade-off between TPR and FPR for every possible probability. It labels the efficiency of vertebral segmentation and also signifies the degree of capability. Higher the rate of ROC denotes better the performance of segmentation approach. The proposed model has obtained the AUC value as 98.5% whereas the existing SEGNET as 96.5%, CNN as 94%, FCM as 92% and OT as 89% in case of reconstructed spine X-ray dataset. From the above figure, it is noticed that AUC generated superior performance in case of proposed model compared with the existing techniques. The time complexity analysis of proposed and existing models is depicted in *figure 10*.

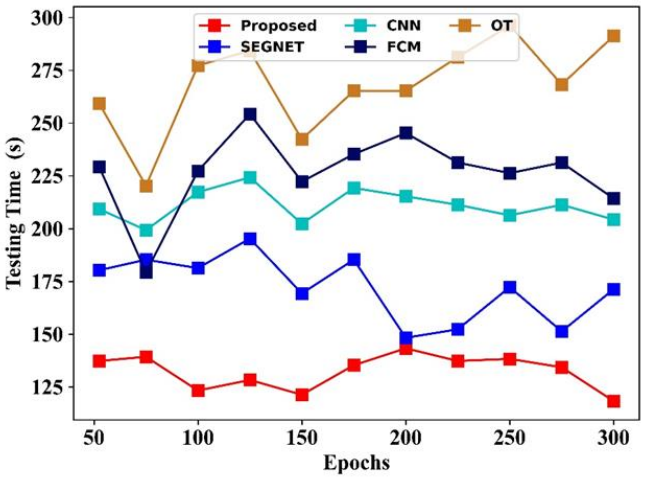

Figure 10: Time complexity analysis

The time complexity signifies the time taken for a model to generate a valuable segmentation outcome. In the proposed work, the time complexity is analysed by varying the epoch size from 50-300. To inspect the proposed performance, the time taken by the existing models like OT, FCM, CNN and SEGNET are compared. The time taken by the proposed Hybrid UDA Net model is 118.3 seconds. The time attained by OT is 291.3 seconds, 214.3 seconds is gotten for FCM, 204.3 seconds are consumed by CNN and 171.3 seconds by SEGNET to perform the segmentation process. From the above graphical representation, it can be perceptibly justified that the proposed model has attained less time complexity because of training most significant features. The performance of dice similarity and RMSE by varying epoch size are depicted in *figure 11 (a)-(b)*.

FOREX Publication
Open Access | Rapid and quality publishing
International Journal of Electrical and Electronics Research (IJEER)
Research Article | Volume 11, Issue 4 | Pages 1225-1239 | e-ISSN: 2347-470X

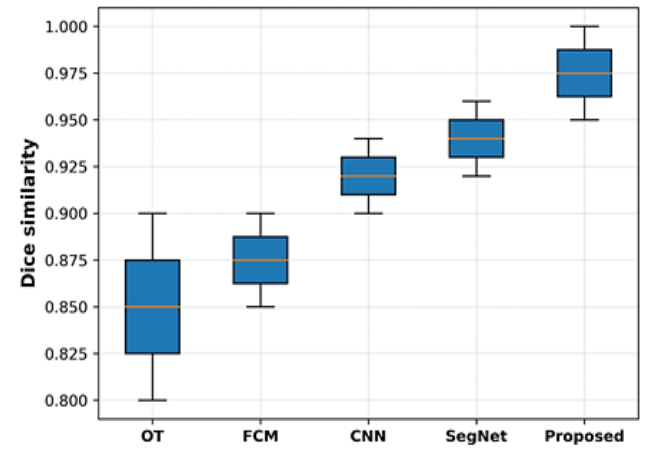

(a)

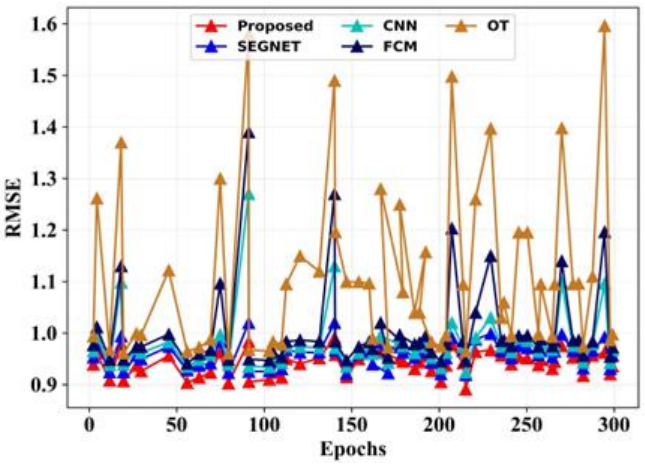

(b)

Figure 11: Proposed and existing comparison (a) Dice similarity (b) RMSE

A clear analysis can be made from the above figure that the dice similarity coefficient of proposed Hybrid UDA Net model in vertebral segmentation has attained improved outcomes compared to the existing models. The dice similarity coefficient of 0.99 is obtained by the proposed model whereas the existing OT has obtained 0.87, FCM as 0.9, CNN as 0.95 and SEGNET as 0.98 respectively. Better similarity is attained by concentrating over the most desirable features through efficient methodologies employed for segmentation. Improved training ability and only negligible errors are observed by processing optimal features. The existing models like OT, FCM, SEGNET and CNN has accomplished less performance than the proposed model because of certain drawbacks like utilization of non-significant features, less training ability and increased training time. On comparing the RMSE values between the proposed and existing models for 300 epochs, the proposed model obtained only lesser RMSE rate of 0.897 whereas OT attained 1.908, FCM as 1.862, CNN as 1.536 and SEGNET as 1.102 respectively.

4.4 Evaluation Measures in Terms of Training and Testing

The accuracy and loss of proposed model is analysed with training and testing data. *Figure 12 (a)-(d)* depicts the accuracy and loss performance attained during diverse stages of proposed model.

By changing the epoch size from 0-300, the accuracy and loss performance of the proposed model are evaluated. The accuracy evaluated for testing and training are almost alike from the above graphical statement. The accuracy increases with increased epoch size whereas the loss decreases with increased epoch size. When the epoch size is increased to 300, an accuracy of 95 to 100% is attained. And from the figure, it is obvious that the proposed model attains maximum accuracy. The training and testing loss is examined for the proposed model and the network has been trained for 300 epochs. If the epoch size is increased to 300, the model obtains a loss in the range between 0.05-0.2. The proposed model gained minimal losses because of effective data training process through Hybrid UDA Net architecture.

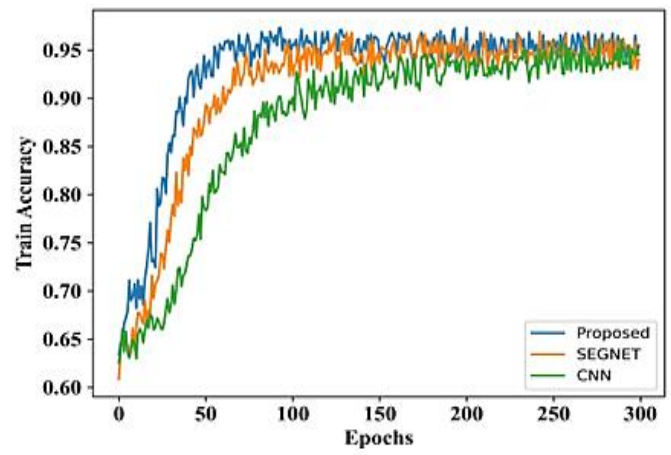

(a)

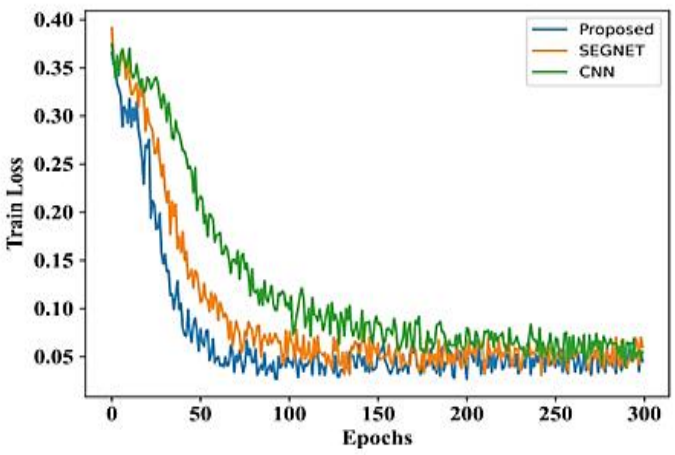

(b)

FOREX Publication
Open Access | Rapid and quality publishing
International Journal of Electrical and Electronics Research (IJEER)
Research Article | Volume 11, Issue 4 | Pages 1225-1239 | e-ISSN: 2347-470X

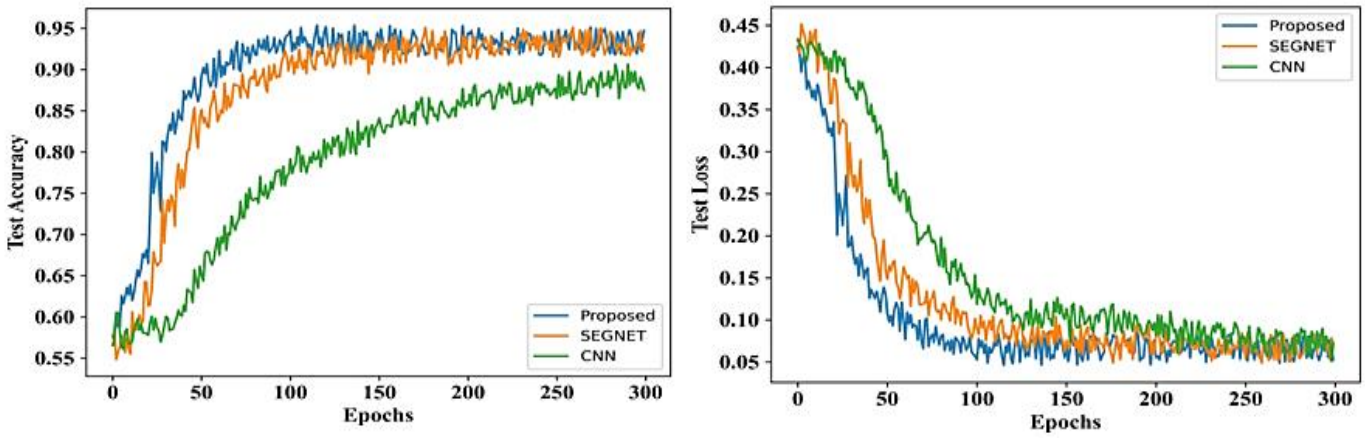

(c) (d)

Figure 12: Performance outcomes (a) Train accuracy (b) Train Loss (c) Test accuracy (d) Test Loss

4.5 Performance Analysis of K-fold Cross Validation

In the proposed research work, K-fold cross validation (K=50) is employed and the performance metrics like accuracy, specificity and F1-score are analysed. Fifty random fold integrations for training and testing are designed in 50-fold cross validation. For 50 times, the proposed techniques get iterated and the segmentation model performs training and testing over every dataset images.

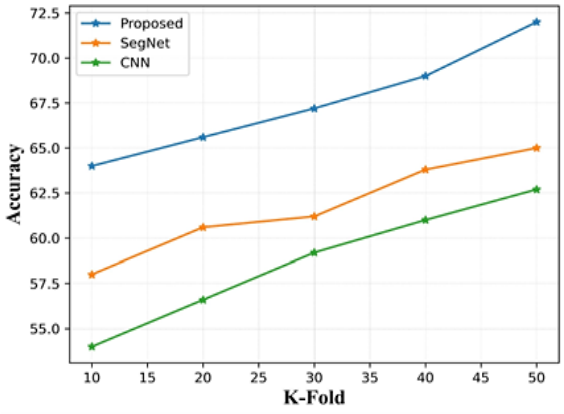

(a)

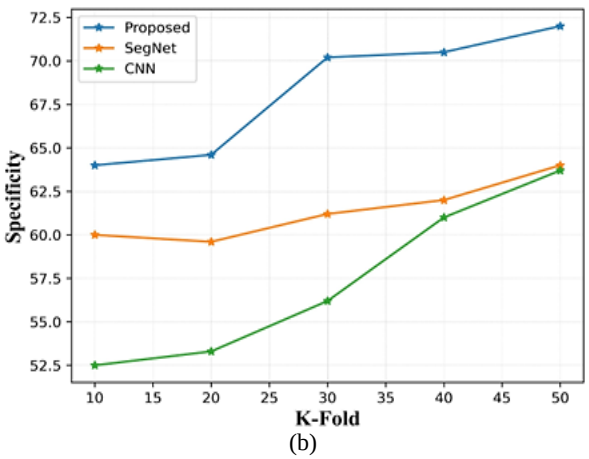

(b)

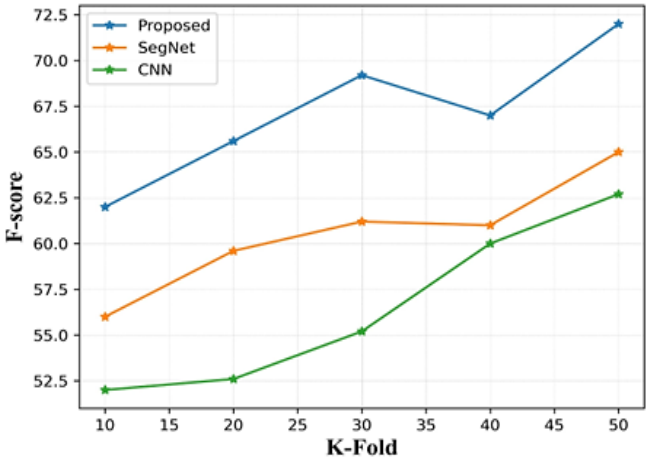

(c)

Figure 13: K-fold analysis (a) Accuracy (b) Specificity (c) F-score

During cross validation, the input dataset is folded in to 50-fold set of reconstructed spine X-ray images. As compared with other techniques, the proposed model obtains better performance for 50-fold cross validation and the performance is varied for all techniques. The analysis of K-fold cross validation is depicted in *figure 13 (a)-(c)*.

4.6 Segmentation Outcomes of Reconstruction Spine X-ray Images

The segmentation results obtained based on the given input images are described in this section. *Figure 14* shows the outcomes of segmented images with the representation of five samples. A set of samples collected from reconstructed Spine X-ray images are given as the input to Hybrid UDA Net architecture for accurate vertebral segmentation. If non-significant features are utilized from the input images, it can lead to inaccurate outcomes which degrade the overall performance. Hence to improve the overall accuracy of proposed model, the effective features are extracted from the encoder section of UNET and the segmented images are obtained from the decoder section of UNET.

FOREX Publication
Open Access | Rapid and quality publishing
International Journal of Electrical and Electronics Research (IJEER)
Research Article | Volume 11, Issue 4 | Pages 1225-1239 | e-ISSN: 2347-470X

Input Image	OT	FCM	CNN	SEGNET	Proposed
 Sample 1					
 Sample 2					
 Sample 3					
 Sample 4					
 Sample 5					

Figure 14: Segmentation outcomes

FOREX Publication
Open Access | Rapid and quality publishing
International Journal of Electrical and Electronics Research (IJEER)
Research Article | Volume 11, Issue 4 | Pages 1225-1239 | e-ISSN: 2347-470X

5. CONCLUSION

On considering the challenges over vertebral segmentation accuracy, time complexity and training ability, a novel methodology called Hybrid UDA Net architecture is proposed in this research article. The chief focus of this research is to segment the vertebral portion from reconstructed spine X-ray images and to evaluate the VCF through VCR analysis. Effective robustness and reliability can be obtained by the proposed model and the overall segmentation performance can be enhanced efficiently through Hybrid UDA Net architecture. The proposed architecture comprises of two sections called encoder and decoder whereas the features are extracted using encoder section of U-net architecture through CaL and HaDQcL mechanisms. In the decoder section of U-Net architecture, the spatial and channel features can be extracted from the decoder attention module. Based on the extracted input features, exact segmentation of spinal images are attained using Twin attention mechanism called GDAM. The network losses in the segmentation network are optimized using APoA strategy. The diverse stages of VCF are finally analysed through VCR evaluation. The overall accuracy of 98.41%, F1 score of 96.75% and specificity of 99% is obtained by the proposed Hybrid UDA Net architecture. On comparison with certain existing models, the proposed model attained better performance outcomes. In future studies, the proposed work can be extended through accurate evaluation of VCF through further enhancement of segmentation network. Also, the hyperparameters of segmentation network model can be effectively tuned.

REFERENCES

[1] Seo, Jae Won, Sang Heon Lim, Jin Gyo Jeong, Young Jae Kim, Kwang Gi Kim, and Ji Young Jeon. "A deep learning algorithm for automated measurement of vertebral body compression from X-ray images." Scientific Reports 11, no. 1 (2021): 1-10.

[2] Alsoof, Daniel, George Anderson, Christopher L. McDonald, Bryce Basques, Eren Kuris, and Alan H. Daniels. "Diagnosis and Management of Vertebral Compression Fracture." The American Journal of Medicine (2022).

[3] Cheng, Pengfei, Yusheng Yang, Huiqiang Yu, and Yongyi He. "Automatic vertebrae localization and segmentation in CT with a two-stage Dense-U-Net." Scientific Reports 11, no. 1 (2021): 1-13.

[4] Li, Bing, Shaoyong Wu, Siqin Zhang, Xia Liu, and Guangqing Li. "Fast Segmentation of Vertebrae CT Image Based on the SNIC Algorithm." Tomography 8, no. 1 (2022): 59-76.

[5] Qadri, Syed Furqan, Linlin Shen, Mubashir Ahmad, Salman Qadri, Syeda Shamaila Zareen, and Muhammad Azeem Akbar. "SVseg: stacked sparse autoencoder-based patch classification modeling for vertebrae segmentation." Mathematics 10, no. 5 (2022): 796.

[6] Yoon, Byung-Ho, Ho Won Kang, Su Min Kim, and Young Do Koh. "Prevalence and Risk Factors of T-Score Spine-Hip Discordance in Patients with Osteoporotic Vertebral Compression Fracture." Journal of Bone Metabolism 29, no. 1 (2022): 43.

[7] Ni, W., C. Ricker, M. Quinn, N. Gasquet, D. Janardhanan, C. J. Gilligan, and J. A. Hirsch. "Trends in opioid use following balloon kyphoplasty or vertebroplasty for the treatment of vertebral compression fractures." Osteoporosis International 33, no. 4 (2022): 821-837.

[8] Ma, Ching-Hou, Hsin-Lun Yang, Yu-Ting Huang, Zhi-Xiang Wu, Hui-Ching Cheng, Wan-Ching Chou, Ching-Hsia Hung, and Kun-Ling Tsai. "Effects of percutaneous vertebroplasty on respiratory parameters in patients with osteoporotic vertebral compression fractures." Annals of Medicine 54, no. 1 (2022): 1320-1327.

[9] Gou, Pengguo, Zhihui Zhao, Chen Yu, Xuefeng Hou, Gang Gao, Ting Zhang, and Feng Chang. "Efficacy of Recombinant Human Parathyroid Hormone versus Vertebral Augmentation Procedure on Patients with Acute Osteoporotic Vertebral Compression Fracture." Orthopaedic Surgery 14, no. 10 (2022): 2510-2518.

[10] Guo, Rui, Bo Li, Ziliang Zeng, Xu Jiang, Di Zhang, Tianyu Xie, Xumin Hu, and Liangbin Gao. "Thoracolumbar kyphosis in postmenopausal osteoporosis patients without vertebral compression fractures." Annals of Translational Medicine 10, no. 2 (2022).

[11] Sozzi, Carlo, Mirko Trentadue, Lisa Nicolì, Federica Tavani, and Enrico Piovan. "Utility of vertebral biopsy before vertebroplasty in patients with diagnosis of vertebral compression fracture." La radiologia medica 126, no. 7 (2021): 956-962.

[12] Feng, Shixiang, Beibei Liu, Ya Zhang, Xiaoyun Zhang, and Yuehua Li. "Two-Stream Compare and Contrast Network for Vertebral Compression Fracture Diagnosis." IEEE Transactions on Medical Imaging 40, no. 9 (2021): 2496-2506.

[13] Chee, Choong Guen, Min A. Yoon, Kyung Won Kim, Yusun Ko, Su Jung Ham, Young Chul Cho, Bumwoo Park, and Hye Won Chung. "Combined radiomics-clinical model to predict malignancy of vertebral compression fractures on CT." European Radiology 31, no. 9 (2021): 6825-6834.

[14] Haffner, Max R., Connor M. Delman, Joseph B. Wick, Gloria Han, Rolando F. Roberto, Yashar Javidan, Eric O. Klineberg, and Hai V. Le. "Osteoporosis Is Undertreated After Low-energy Vertebral Compression Fractures." JAAOS-Journal of the American Academy of Orthopaedic Surgeons 29, no. 17 (2021): 741-747.

[15] Liu, Cheng, and Cuili Shu. "Vertebral Compression Fractures—The First Manifestations in the Elderly Acute Lymphoblastic Leukemia." Geriatric Orthopaedic Surgery & Rehabilitation 12 (2021): 21514593211026803.

[16] Qi, Haoran, Jun Qi, Junying Gao, Jianmin Sun, and Guodong Wang. "The impact of bone mineral density on bone metabolism and the fracture healing process in elderly Chinese patients with osteoporotic vertebral compression fractures." Journal of Clinical Densitometry 24, no. 1 (2021): 135-145.

[17] Yilmaz, Eren Bora, Christian Buerger, Tobias Fricke, Md Motiur Rahman Sagar, Jaime Peña, Cristian Lorenz, Claus-Christian Glüer, and Carsten Meyer. "Automated deep learning-based detection of osteoporotic fractures in CT images." In International Workshop on Machine Learning in Medical Imaging, pp. 376-385. Springer, Cham, 2021.

[18] Yasaka, Koichiro, Hiroyuki Akai, Akira Kunimatsu, Shigeru Kiryu, and Osamu Abe. "Prediction of bone mineral density from computed tomography: application of deep learning with a convolutional neural network." European radiology 30, no. 6 (2020): 3549-3557.

[19] Monchka, Barret A., John T. Schousboe, Michael J. Davidson, Douglas Kimelman, Didier Hans, Parminder Raina, and William D. Leslie. "Development of a manufacturer-independent convolutional neural network for the automated identification of vertebral compression fractures in vertebral fracture assessment images using active learning." Bone 161 (2022): 116427.

[20] Dong, Qifei, Gang Luo, Nancy E. Lane, Li-Yung Lui, Lynn M. Marshall, Deborah M. Kado, Peggy Cawthon et al. "Deep Learning Classification of Spinal Osteoporotic Compression Fractures on Radiographs using an Adaptation of the Genant Semiquantitative Criteria." Academic radiology (2022).

[21] Monchka, Barret A., Douglas Kimelman, Lisa M. Lix, and William D. Leslie. "Feasibility of a generalized convolutional neural network for automated identification of vertebral compression fractures: The Manitoba Bone Mineral Density Registry." Bone 150 (2021): 116017.

[22] Kong, Sung Hye, Jae-Won Lee, Byeong Uk Bae, Jin Kyeong Sung, Kyu Hwan Jung, Jung Hee Kim, and Chan Soo Shin. "Development of a spine X-ray-based fracture prediction model using a deep learning algorithm." Endocrinology and Metabolism 37, no. 4 (2022): 674-683.

[23] Hu, Xiao, Yanjing Zhu, Yadong Qian, Ruiqi Huang, Shuai Yin, Zhili Zeng, Ning Xie et al. "Prediction of subsequent osteoporotic vertebral

compression fracture on CT radiography via deep learning." View (2022): 20220012.

[24] Iyer, Sankaran, Arcot Sowmya, Alan Blair, Christopher White, Laughlin Dawes, and Daniel Moses. "A novel approach to vertebral compression fracture detection using imitation learning and patch based convolutional neural network." In 2020 IEEE 17th International Symposium on Biomedical Imaging (ISBI), pp. 726-730. IEEE, 2020.

[25] Seo, Jae Won, Sang Heon Lim, Jin Gyo Jeong, Young Jae Kim, Kwang Gi Kim, and Ji Young Jeon. "A deep learning algorithm for automated measurement of vertebral body compression from X-ray images." Scientific Reports 11, no. 1 (2021): 1-10.

[26] Wu, Hongbo, Chris Bailey, Parham Rasoulinejad, and Shuo Li. "Automatic landmark estimation for adolescent idiopathic scoliosis assessment using BoostNet." In International Conference on Medical Image Computing and Computer-Assisted Intervention, pp. 127-135. Springer, Cham, 2017.